Model Identification of a Spatiotemporally Varying Catalytic Reaction

K. Krischer, R. Rico-Martínez, and I. G. Kevrekidis
Dept. of Chemical Engineering, Princeton University, Princeton, NJ 08544

H. H. Rotermund and G. Ertl
Fritz-Haber-Institut der Max-Planck-Gesellschaft, Faradayweg 4-6, W-1000 Berlin 33, Germany

J. L. Hudson
Dept. of Chemical Engineering, University of Virginia, Charlottesville, VA 22093

The occurrence of instabilities in chemically reacting systems, resulting in unsteady and spatially inhomogeneous reaction rates, is a widespread phenomenon. In this article, we use nonlinear signal processing techniques to extract a simple, but accurate, dynamic model from experimental data of a system with spatiotemporal variations. The approach consists of a combination of two steps. The proper orthogonal decomposition [POD or Karhunen-Loève (KL) expansion] allows us to determine active degrees of freedom (important spatial structures) of the system. Projection onto these "modes" reduces the data to a small number of time series. Processing these time series through an artificial neural network (ANN) results in a low-dimensional, nonlinear dynamic model with almost quantitative predictive capabilities.

This approach is demonstrated using spatiotemporal data from CO oxidation on a Pt(110) crystal surface. In this special case, the dynamics of the two-dimensional reaction profile can be successfully described by four modes; the ANN-based model not only correctly predicts the spatiotemporal short-term behavior, but also accurately captures the long-term dynamics (the attractor). While this approach does not substitute for fundamental modeling, it provides a systematic framework for processing experimental data from a wide variety of spatiotemporally varying reaction engineering processes.

Introduction

Chemically reacting systems often develop instabilities and operate under unsteady and/or spatially nonuniform conditions. Spatially nonuniform processes are in principle characterized by an infinite number of "modes" or "degrees of freedom," and are usually modeled by partial differential equations (PDEs). On the other hand, it is often observed that, after the initial transients decay, the long-term dynamics of many reacting systems are inherently "low-dimensional"; in our context this means that they appear qualitatively similar to the dynamics of a small set of ODEs. In such cases, it should in principle be possible to describe the dynamics of the system by the temporal evolution of a small set of *appropriately chosen* variables. A successful reduction of the system dimension seems

therefore to be an essential step for modeling and identification tasks in systems exhibiting spatiotemporal variations.

In this article we use available experimental information to both reduce the data, and subsequently identify an *ad hoc* low-dimensional accurate dynamic model of a heterogeneously catalyzed reaction. The approach is based on the availability of detailed (spatiotemporal) experimental data, and it is a combination of two steps. The first step is based on traditional statistical techniques [principal factor analysis or Karhunen-Loève (KL) expansion]. This approach has been used in the weather prediction context (for example, Lorenz, 1956), as well as in the context of identifying coherent spatial structures in time-dependent hydrodynamics by Lumley (1967), who re-

ferred to it in the latter context as the proper orthogonal decomposition (POD). The main idea is to identify coherent spatial structures by diagonalizing the covariance or two-point correlation matrix obtained from the experimental data. More recently, Sirovich and his coworkers (Sirovich, 1987; Sirovich and Sirovich, 1989) pointed out that the temporal correlation matrix will yield the same dominant spatial modes, while often giving rise to a much smaller (and thus computationally more tractable) eigenproblem ("method of snapshots"). The identification of such active spatially coherent modes provides insight in the spatial structure and the instabilities, and is therefore an important task in itself (see, for example, Aubry et al., 1991). But the modes can also be used as an optimal set of basis functions to obtain a low dimensional model (in a Galerkin projection, see Deane et al., 1991, and references therein) provided that a fundamental model is available. For many practical applications in chemical systems, however, phenomenological models are often inaccurate, or are not robust enough to predict experimental data accurately. In such cases, characterizing and predicting the dynamics can still be achieved with *ad hoc* dynamic models, like the ones obtained using artificial neural networks. [See, for example, Lapedes and Farber (1987), and in the chemical engineering literature McAvoy et al. (1989) or Hudson et al. (1990) among others.]

In addition to this, the KL expansion has been used as a basis for the control of distributed parameter systems by Gay and Ray (1986, 1988) and by Chang and his coworkers (Chen et al., 1990; Chen and Chang, 1992). In the latter reference they also include an application of the procedure to spatio-temporal experimental data of temperature variations on a catalytic wafer (Kellow and Wolf, 1991).

We illustrate here through an experimental example that the combination of the KL expansion with nonlinear signal processing using ANNs is a promising approach for the identification and characterization of the dynamic behavior of systems for which models based on first principles are unavailable or not sufficiently quantitative. The approach obviously does not substitute for true understanding of the underlying physicochemical mechanisms, since only a "black box" model of the dynamics is constructed. In addition, as will be seen below for our example, the general shape of the spatial modes is not exclusively characteristic of the CO oxidation reaction nor does it directly reflect the geometry of the underlying Pt crystal surface; such shapes could naturally occur—possibly with different wavelength—in other pattern forming systems. In this context, the procedure should be thought of as a good data post-processing tool: it is helpful in understanding and predicting certain features of the *dynamic behavior* of the system. Even without fundamental understanding of the physiochemical mechanisms causing the dynamics, the procedure leads to low dimensional input-output models. Such models are useful in identifying the underlying bifurcations, as well as in real-time prediction and modal feedback control or model-predictive control of the distributed system (possibly with on-line updating of the KL modes and/or the dynamic model). If, on the other hand, a detailed, quantitatively accurate fundamental model of the process is available, the experimentally determined KL modes can still assist in reducing the dimension of traditional discretizations of the PDE: using these modes in a Galerkin expansion can again yield an accurate, low-dimensional model, combining first principles modeling (the PDE)

with experimental information (the choice of modes). Such models can be used during mechanistic studies by assisting the validation of fundamental PDE models: it is much easier to computationally explore the predictions of a few ODEs rather than large-scale traditional PDE discretizations. They can, of course, also be used for real-time prediction and/or modal control in lieu of the more *ad hoc* models constructed using ANNs or other black-box methods.

The experimental data used here come from a heterogeneous gas-phase reaction, the CO oxidation on Pt (110). This system has been known for many years to exhibit a rich variety of oscillatory behavior in the overall reaction rate (Ertl, 1990; Eiswirth et al, 1990). More recent experiments show that most of these temporal oscillations are accompanied by the formation of spatial patterns (Jakubith et al., 1990).

In this article, we discuss briefly the spatio-temporal data and the KL expansion, as well as its usefulness for obtaining a low-dimensional representation of the data. Then, using the reduced data set to train an ANN, we show that the resulting nonlinear model is capable of accurately predicting the short-term and even the long-term dynamics of the distributed system.

Experimental Data: Periodic Patterns in the CO Oxidation on Pt (110)

The images produced in Figure 1 show one type of spatio-temporal patterns found during the oxidation of CO on a Pt (110) single crystal surface under low pressures. They were obtained with a photoemission electron microscope (PEEM) which monitors differences of the work function ϕ of the surface. Adsorption of either CO or O_2 on a Pt (110) crystal leads to an increase of ϕ. The effect chemisorption of O_2 has on ϕ, however, is nearly twice as large as the one of a CO saturated surface. In the pseudocolor representation of Figure 1, regions covered mainly with oxygen appear blue, while the red areas indicate predominantly CO-covered regions; green and yellow colored areas symbolize medium and low oxygen coverages. A review of the chemical processes which occur during this reaction, the mechanism leading to the instability, as well as a survey of the different phenomena and a detailed description of the experimental setup, may be found elsewhere (Ertl, 1990; Rotermund et al., 1991).

The first five images in Figure 1 show snapshots of the surface during half an oscillation period. The CO-covered (red) areas of the first image continuously convert into regions where oxygen is predominantly adsorbed (images 4 and 5), and *vice versa*: regions which in the first picture are oxygen-covered (blue) evolve into CO-covered states. The periodicity of the pattern in space apparently leads to some sort of symmetry: a lateral shift of image 1 by half a spatial wavelength converts it into image 5. Image 6 shows the surface after one full oscillation. The system has returned to the initial state of this sequence (image 1).

The temporal evolution of the pattern is visualized more clearly in Figure 2A where a horizontal cut through the pattern is shown as a function of time over approximately 2.5 periods. The horizontal white bar in the first image of Figure 1 indicates where the cut was taken. In this representation, the shift of the pattern by half a spatial wavelength after half a period in time can be seen more clearly; it becomes completely evident
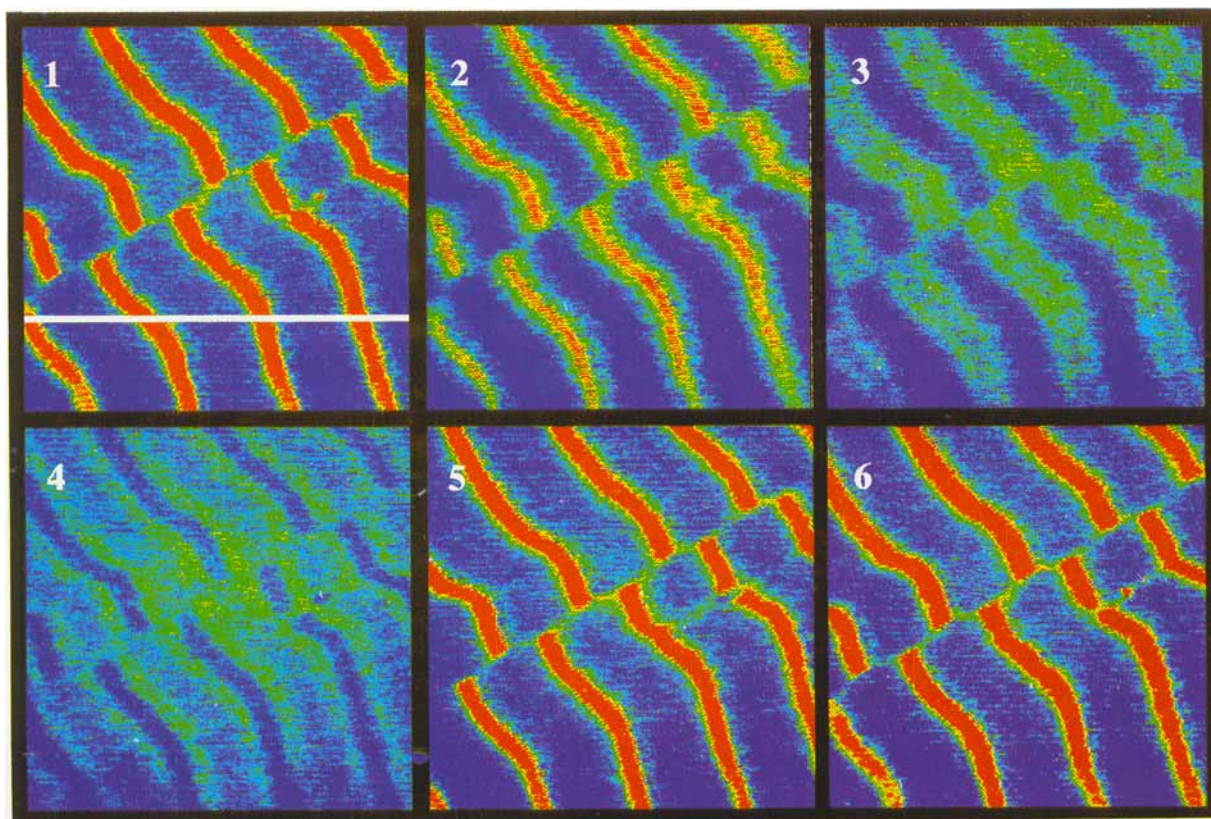
Figure 1. Sequence of images obtained during the CO oxidation on an approximately 300 × 300 μm² section of a Pt(110) surface at $T = 550$ K, $P_{O_2} = 4.1 \times 10^{-4}$ mbar and $P_{CO} = 1.75 \times 10^{-4}$ mbar.

The time interval between the first and subsequent five images is: 6/30, 8/30, 11/30, 23/30, and 44/30 s. Images are taken from a fluorescence screen by a CCD video camera and stored on video tape. The arbitrary gray-scale tape was digitized for the calculations. Pseudocolors were used to enhance the contrast between predominantly oxygen covered (blue) and CO covered (red) regions. The white bar in image 1 indicates where the data in Figure 2 and underlying Figure 7 were taken.
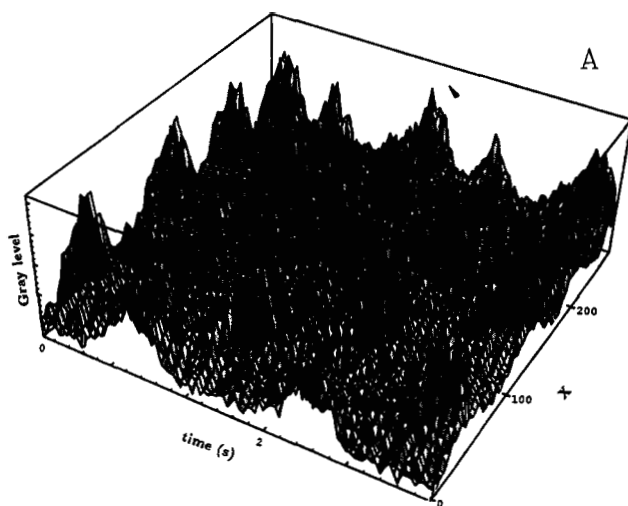

**Figure 2A. Temporal evolution of the "slice" indicated in Figure 1 (image 1).**

About 2.5 periods are shown. The spatial coordinate is given in "pixel" units (1 pixel is approximately equal to 1.2 μm). The amplitude is a measure of the work function (that is, the adsorbate coverages) (arbitrary units).

in Figures 2B and 2C where the time series obtained at two points located half a wavelength apart are shown.

In Figure 1 each image is represented by 256 * 256 numbers (pixels) and can be thought of as a 256 * 256-long vector, or a point in R^{65536}. As we discussed in the introduction section, however, the dynamics of distributed chemically reacting sys-
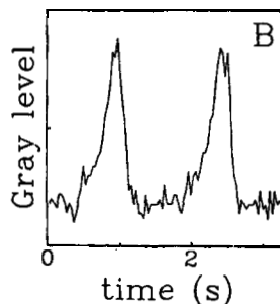
Figure 2B. Time series of the amplitude at $x = 80$.
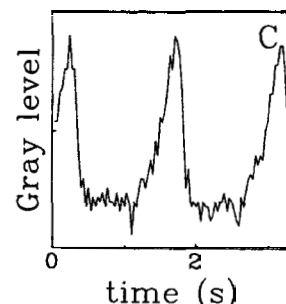
Figure 2C. Time series of the amplitude at $x = 122$.

The latter is taken half a spatial period apart from the one in Figure 2B. Note the phase shift of $T/2$ compared to Figure 2B.

tems often live in a low-dimensional subspace of the phase space. The data presented in this section exhibit a high degree of spatial order, indicating that the dynamics could indeed be successfully described by a low-dimensional model.

Data Reduction with the Karhunen-Loève Expansion

Given a set of spatially varying data (an ensemble of instantaneous "snapshots") which were collected at M instants in time, we start by writing the state variables as deviations from their ensemble average $\langle U(x) \rangle$:

$$U(x, t) = \langle U(x) \rangle + u(x, t), \quad \langle u(x, t) \rangle = 0 \quad (1)$$

If U is known at N discrete points in space, the elements r_{ij} of the two-point correlation matrix R are defined as:

$$r_{ij} = \frac{1}{M} \sum_{m=1}^{M} [u(x_i, t_m) u(x_j, t_m)] \quad i, j = 1, \ldots, N \quad (2)$$

The (normalized) eigenvectors ϕ_i of the matrix R form a complete orthonormal set, and the corresponding eigenvalues λ_i quantify the probability of their occurrence in the data in the sense:

$$\lambda_i = \langle (u, \phi_i)^2 \rangle \quad (3)$$

or, equivalently, the mean "energy" of the data projected on the ϕ_i axis. Here, the parentheses denote the inner product and the angle brackets the ensemble average.

The state of the system at any instant can then be represented in terms of these eigenfunctions ("coherent structures") ϕ_i:

$$u(x, t) = \sum_{j=1}^{M} C_j(t) \phi_j(x) \quad (4)$$

The coefficients C_i are obtained by projecting the data onto the eigenvectors:

$$C_i(t) = (\phi_i(x), u(x, t)) \quad (5)$$

and are uncorrelated in time.

In distributed systems with two or three spatial dimensions the size of the covariance matrix (2) might make the direct computational evaluation of the eigenvalue problem prohibitive. [In our example, the matrix has $O(10^9)$ elements.] If a few hundred snapshots can provide a good description of the dynamics, however, the eigenfunctions may be readily calculated via diagonalization of the temporal correlation matrix A:

$$A_{mn} = \frac{1}{M} (u_m(x), u_n(x)) \quad (6)$$

$$Ab = \lambda b \quad (7)$$

$$\phi_i(x) = \sum_{m=1}^{M} b_{m,i} u_m(x) \quad (8)$$

Table 1. Individual and Cumulative Energy Captured by the First Few Modes

| Mode No.	Normalized Energy	Cumulative Normalized Energy
1	0.6670	0.6670
2	0.1640	0.8310
3	0.0309	0.8619
4	0.0173	0.8792
5	0.0084	0.8876
6	0.0062	0.8938
7	0.0042	0.8980
.		
15	0.0011	0.9106
.		
.		
20	0.0008	0.9149

This has been termed "the method of snapshots" (Sirovich, 1987).

For the determination of the "coherent structures" from the experimental data of Figure 1, we used 500 snapshots (over approximately 11 periods), each snapshot consisting of $256 * 256$ values or pixels. As noted above, before decomposing the matrix, the temporal average was subtracted. Table 1 shows the seven largest normalized eigenvalues together with their cumulative contribution to the total "energy." The first mode already captures 2/3 of the total energy and the first four modes collectively carry 88%. The contribution of the higher modes to the energy becomes considerably smaller, so that taking into account 15 (resp. 20) modes leads only to a small increase of the captured energy to 91.1% (resp. 91.5%). The presence of a large number of modes with a negligible contribution to the total energy may be attributed to noise without any "preferred" direction. Neglecting the contribution of those modes may thus be regarded as a filtering procedure.

The first four coherent structures are shown in Figure 3A. The stripe-like pattern of the original data is clearly visible in these vectors and, at first glance, perpendicular to the stripes, the eigenmodes ϕ_1-ϕ_3 are reminiscent of Fourier modes: they are fairly periodic in space, and the second (third) vector has a spatial frequency which is twice (three times, respectively) the spatial frequency of the first one. As can be seen more clearly in Figure 3B, where cuts through the vectors (taken at the same location which is indicated in Figure 1) are shown, the shape of the modes is obviously nonsinusoidal, the amplitudes vary in height, and the mean is different from zero. The KL expansion ensures that these basis functions are optimal in a least-square sense in representing the particular data; they are clearly superior in capturing the data to an equal number of Fourier modes. While we here have concentrated on data from a particular surface "patch," geometrically similar shapes are observed over the entire macroscopic (centimeter scale) surface. In general, we expect geometric features (for example, symmetries) of the underlying domain to be apparent in the modes themselves.

A comparison of the first four original snapshots in Figure 1 with the corresponding reconstructed ones using four modes (Figure 4) show a remarkable agreement of the two representations. This indicates that the dynamics of the spatiotemporal data indeed lives in a low-dimensional subspace of the 65,536-dimensional phase space, and that the KL expansion indeed
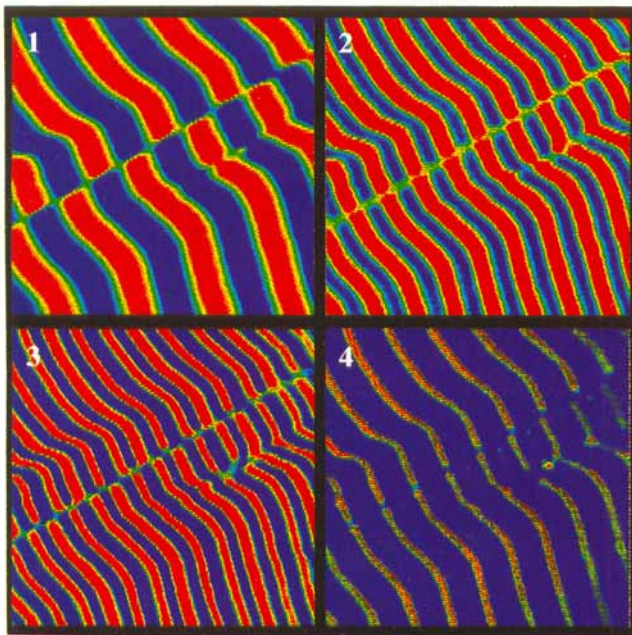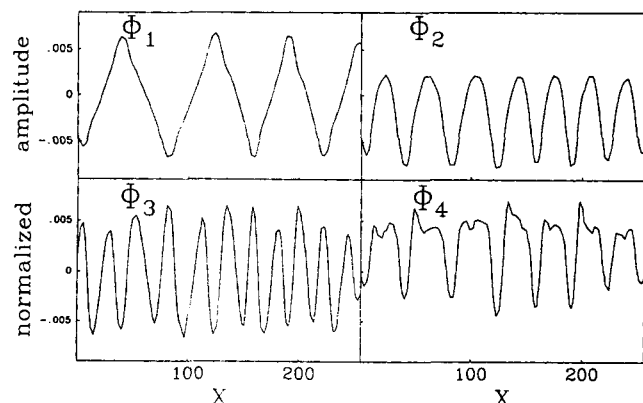
Figure 3A. First four coherent structures.

Note that the spatial periods between ϕ_1 and ϕ_2, ϕ_3, and ϕ_4 have ratios of 1:2, 1:3 and 1:2, respectively.

Figure 4. Reconstructions of the spatial patterns using the first four modes.

The images correspond to the first four images in Figure 1.

provides a set of appropriate basis vectors which span this subspace. Moreover, collating Figure 1 and Figure 4 again, it is evident that the noise which seems to be most pronounced in the horizontal direction in Figure 1, has been filtered in the reconstructed data.

Projections of the full dynamics onto the first four modes are reproduced in Figure 5. Though the temporal variation of the coefficients of the fourth mode is somewhat noisy, it is evident that all coefficients vary periodically in time. The period of the individual time series, however, is different. C_2 and C_4 apparently oscillate with twice the frequency of C_1, while C_3 exhibits three oscillations during one period of C_1. After one period of the C_1 oscillation, all amplitudes return to their original values and therefore the motion of the experimental data lies on a limit cycle.

As was discussed earlier, the data apparently exhibit a certain spatiotemporal symmetry (images 1 and 5 in Figure 1, which

are half a temporal period apart, seem to be convertible into each other by a spatial shift of half a wavelength). If such a symmetry exists, it also manifests itself in the time series of the coefficients, as well as in the attractor itself. Figure 6 shows

Figure 3B. Cuts through the modes in Figure 3A.

The cuts were taken at the same location indicated in Figure 1.
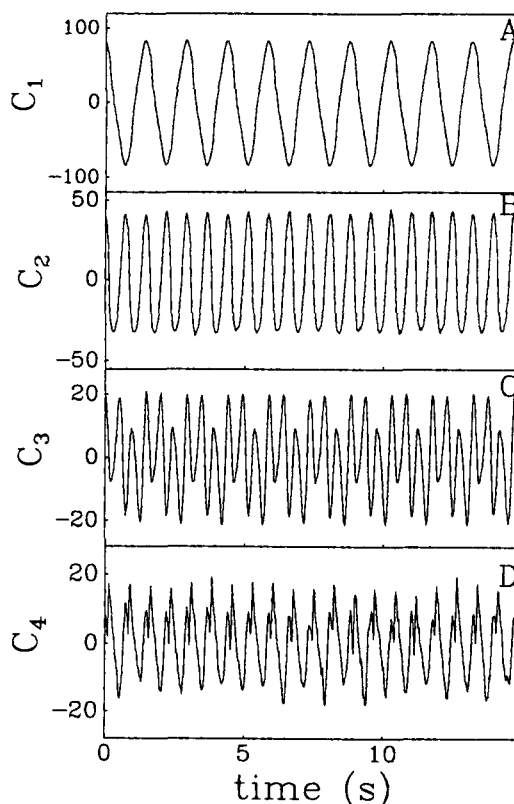
Figure 5. Time series of coefficients of (projections of the data onto) the first four modes.
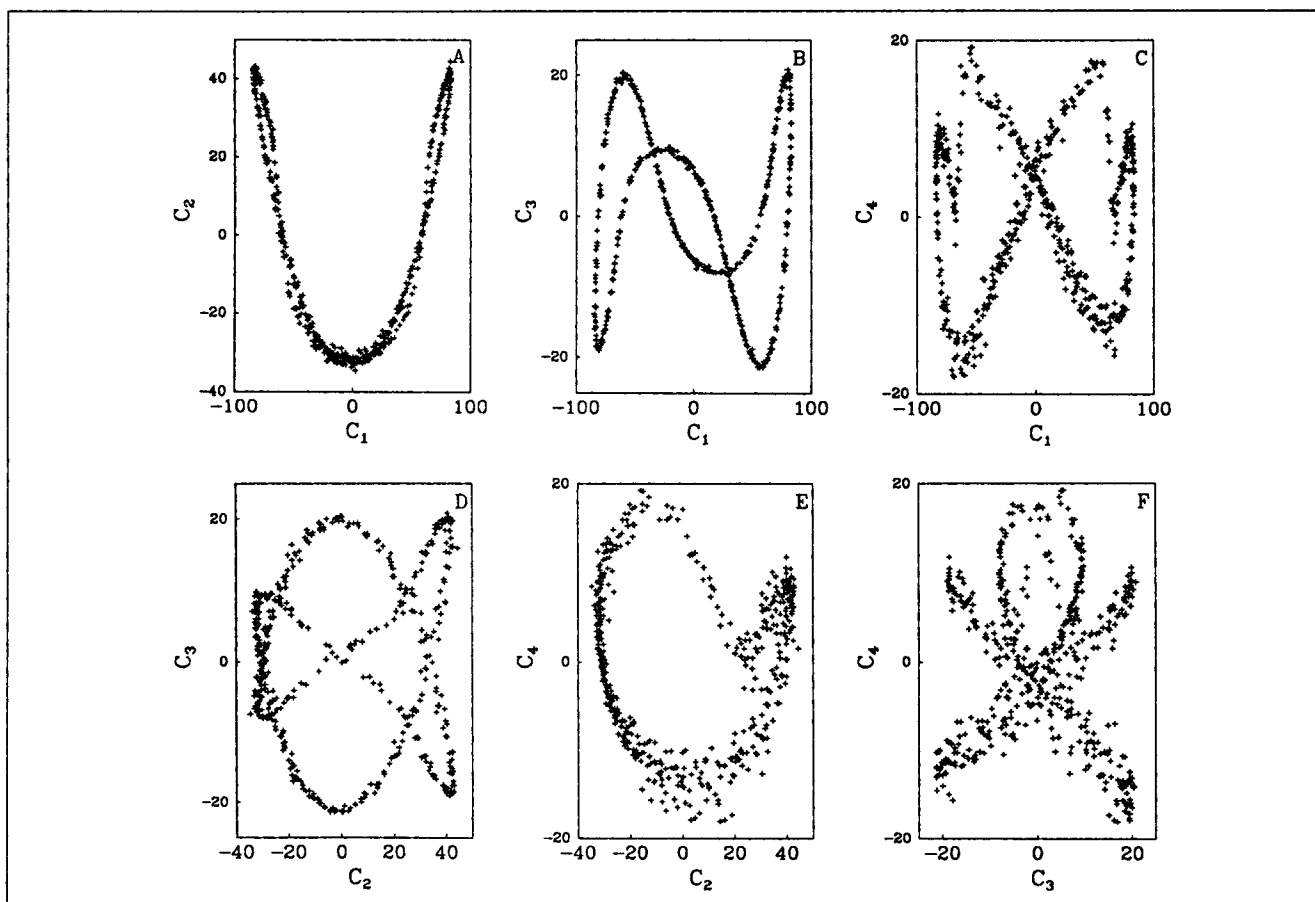
**Figure 6. Six different projections of the experimental atttractor.**

The symmetry properties of the projections are discussed in the text.

six different projections of the attractor, which seem to be symmetric (allowing for some experimental noise). For example, the projections onto the C_1-C_2 and C_1-C_4 planes possess the mirror plane $C_1 = 0$; the projection onto the C_2-C_3 plane is symmetric with respect to a reflection around $C_3 = 0$ and the projection onto the C_1-C_3 plane is invariant upon consecutive reflections around $C_1 = 0$ and $C_3 = 0$. Geometric symmetries inherent in a problem can be exploited to augment the experimental data (Sirovich, 1987); in our case, shifting each snapshot by half a spatial wavelength would give a "legitimate" snapshot (a snapshot that could be experimentally observed). The effect of symmetries, their use in augmenting the data, and their effect on the nature of the modes have recently been discussed by Aubry et al. (1992). We chose here to work with the particular experimental snapshot sequence, and the modes we find are, therefore, tailored to it. In a more general setting, our system could be thought of as translationally invariant in two directions (if we think of the crystal surface as being very large compared to the pattern we study, so that we effectively have periodic boundary conditions). *Any* spatial shift along these directions would then provide "legitimate" snapshots. We will discuss this issue in detail elsewhere.

To a first approximation, the pattern seems to be invariant parallel to the stripes, suggesting that the phenomenon is really one-dimensional. For that reason, we also processed one-dimensional data, obtained by taking a cut through the images (see Figures 1 and 2). In this case, the decomposition was based on 700 snapshots, and each spatial slice was represented by 256 values. The resulting eigenvectors (Figure 7A) were, as expected, very similar to cuts through the corresponding two-dimensional modes (Figure 3B). Accordingly, projections of the one-dimensional reaction profiles onto the one-dimensional modes (Figure 7B) result in time series very similar to, albeit somewhat noisier than, those obtained from the two-dimensional projections (compare with Figure 5). The results show that the dynamics of the stripes themselves can be understood in a one-dimensional framework, whereas obviously other features like orientation of the stripes with respect to the crystallographic directions, dislocations, or the wavy fine structure parallel to the stripes can be described only if one takes into account two spatial dimensions.

So far we have demonstrated that the spatiotemporal evolution of the snapshots can be adequately represented by four time series (the temporal evolution of the coefficients of the four most energetic coherent spatial modes). In a sense, we have successfully compressed the experimental data. We now proceed to construct a low-dimensional model, able to perform accurate predictions of the long-term behavior (the attractor).

Figure 8. Feedforward ANN architecture used.
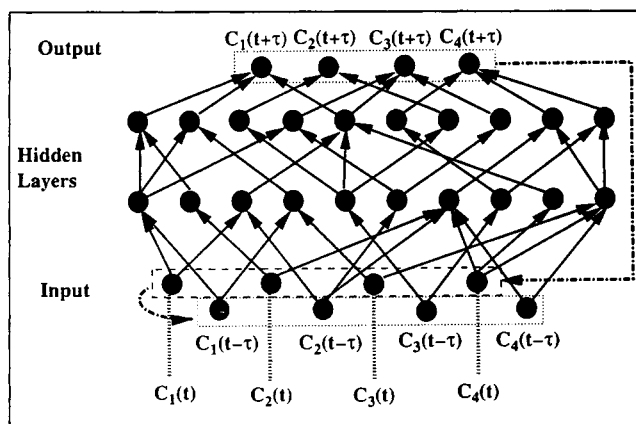
The layers are fully interconnected.
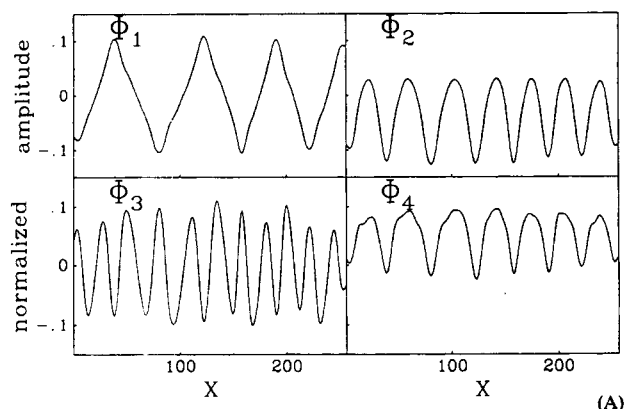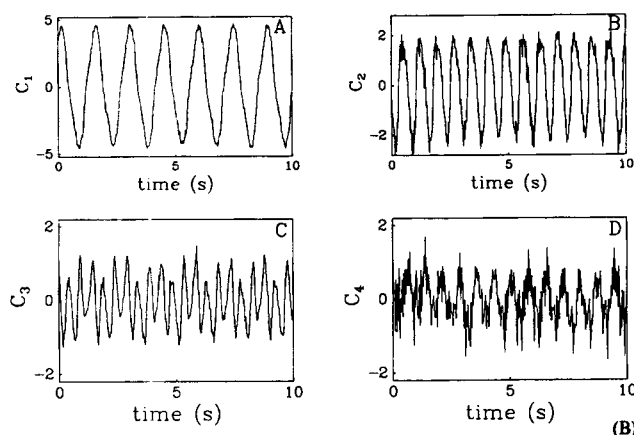
Figure 7. (A) Eigenmodes (ϕ_i) and (B) projections of the dynamics onto them (C_i) for one-dimensional reaction profiles ($i = 1, 2, 3, 4$).

One-dimensional data were obtained by taking a cut through the full images at the location marked in Figure 1.

Artificial Neural Network-Based Low-Dimensional Model

The potential of ANNs for the processing of nonlinear time series, particularly for the prediction of temporally complicated dynamics, has been illustrated by Lapedes and Farber (1987). We, among others, have subsequently tested their ability to identify long-term dynamic behavior and experimentally observed bifurcations (Hudson et al., 1990; Rico-Martínez et al., 1992). Here, we used a two-hidden-layer, feedforward ANN to obtain a dynamic model for our spatially distributed system. As the behavior of the system can be adequately described by four time-dependent coefficients of spatially coherent modes, these time series can be used to train the ANN. In the case discussed below, the ANN input consisted of the values of these four coefficients C_i at time t_n and at time t_{n-1}; $t_{n-1} = t_n - \tau$, where τ was chosen to be 0.1 s, or about 1/10 of a period of C_1. Compared with a net with only four inputs (the values of the coefficients at time t_n only), this architecture, where the input was embedded in an eight dimensional space— exploiting the time-delay method of Packard et al. (1980) and of Takens (1981)—showed better results. The output of the ANN constitutes a prediction of the values of the coefficients C_i at a future time t_{n+1}, that is, we have the following mapping:

$$C_i(t_{n+1}) = F[C_j(t_n), C_j(t_{n-1})] \quad i, j = 1, \dots, 4 \quad (9)$$

where F is a set of nonlinear functions representing the ANN-based model. When (and if) the training coverges, the network approximates a low-dimensional dynamical model of the system, whose state variables are the coefficients of the first four KL eigenmodes. The transformation back to physical space can simply be performed with Eq. 4.

We use a standard (Lapedes and Farber, 1987) ANN architecture consisting of four layers: an eight neuron input layer, two hidden layers with ten neurons each and a four neuron output layer (a schematic is shown in Figure 8). All layers are fully interconnected. The input and output neurons are linear, while the neurons in the hidden layer are nonlinear with a sigmoidal activation function given by $g(X) = 1/2$ $[1 + \tanh(X)]$. As already mentioned, the ANN was trained to predict the state of the system with a prediction horizon of 0.1 s. The training was carried out using conjugate gradients on a total of 300 (temporal) experimental "points"; each "point" consists of eight measurements and four target values. The remaining data points were used during the validation of the training process. The training was considered to be successful when both the mean square prediction error and its rate of decrease fell below preset bounds. In this particular case, training was completed after $O(10^2)$ complete conjugate gradient cycles.

If a net is iterated *ad infinitum* by feeding its output back to the input, the long-term behavior or attractor of the ANN-based model is obtained. In Figure 9 the long-term dynamics of our ANN-based model is shown together with segments of the original time series. The solid line in Figure 9 represents the ANN output, while the crosses show the original data. Reconstructions of the full spatiotemporal behavior (using the coefficients from the long-term ANN predictions) are reproduced in Figure 10. From Figures 9 and 10 it is obvious that the net predicts a *stable* solution with the qualitative features of the training data, and moreover, it even quantitatively captures amplitudes and periods. The projections of the predicted attractor (Figure 11) confirm that the ANN-based model not only restricts the motion to the correct region in phase space but also correctly reproduces the above discussed symmetry of the attractor (modulo, again, some noise: compare Figure 11 and Figure 6).

While the temporal dependence of the data analyzed here
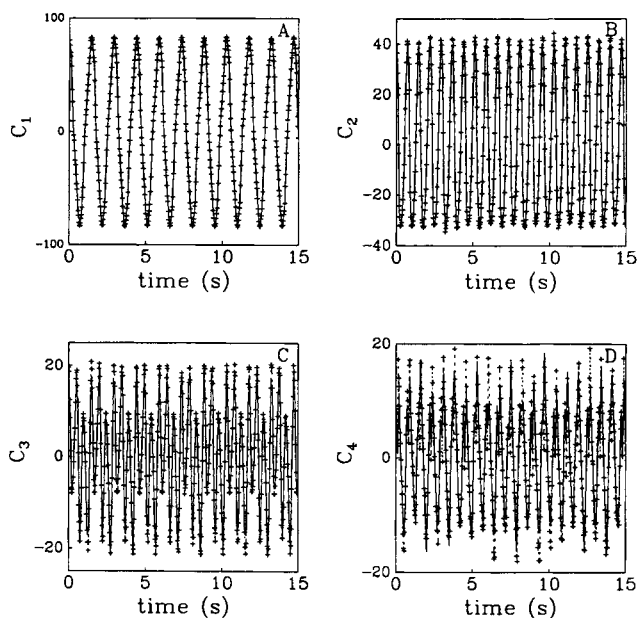
Figure 9. Long-term prediction of the ANN-based network (solid line) vs. original time series (crosses).

is comparatively simple, that is, the signal is periodic, the method is directly applicable to more complicated, even chaotic, dynamics. Furthermore, the dependence of the dynamics on one or more parameters can be easily incorporated in the approach (see, for example, Hudson et al., 1990). It is worth mentioning, however, that certain bifurcation problems can be represented more accurately by ANN architectures capable of fitting a continuous-time model (a set of ODEs) rather than a discrete mapping, an approach discussed in detail by Rico-Martínez et al. (1992).

Summary

We have shown that prediction and characterization of the spatiotemporal dynamics of an experimental system [CO oxidation on Pt (110) under certain conditions] can be achieved with the combination of two methods, data reduction using the Karhunen-Loève expansion, and subsequent construction of an artificial neural network-based dynamic model. When the behavior is inherently low-dimensional, and given experimental data, this approach can lead to comparatively simple models containing only a few variables, but it certainly does not substitute for a fundamental understanding of the underlying physical or chemical mechanisms. Nevertheless, the approach should provide a powerful tool both for understanding
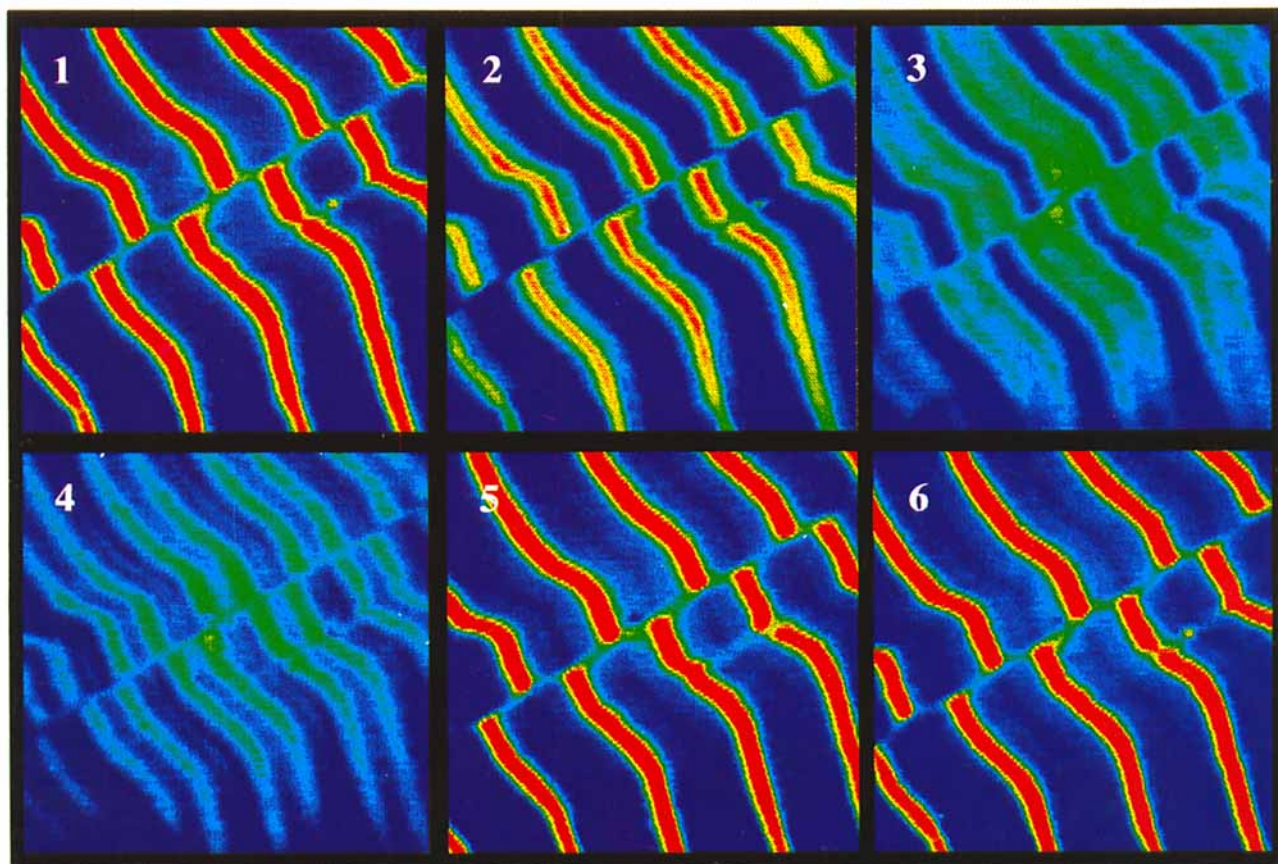
Figure 10. Reconstructions of the two-dimensional patterns from predicted coefficients.

These are long-term predictions and the images represent snapshots taken at the same phase of the oscillations as those in Figure 1.
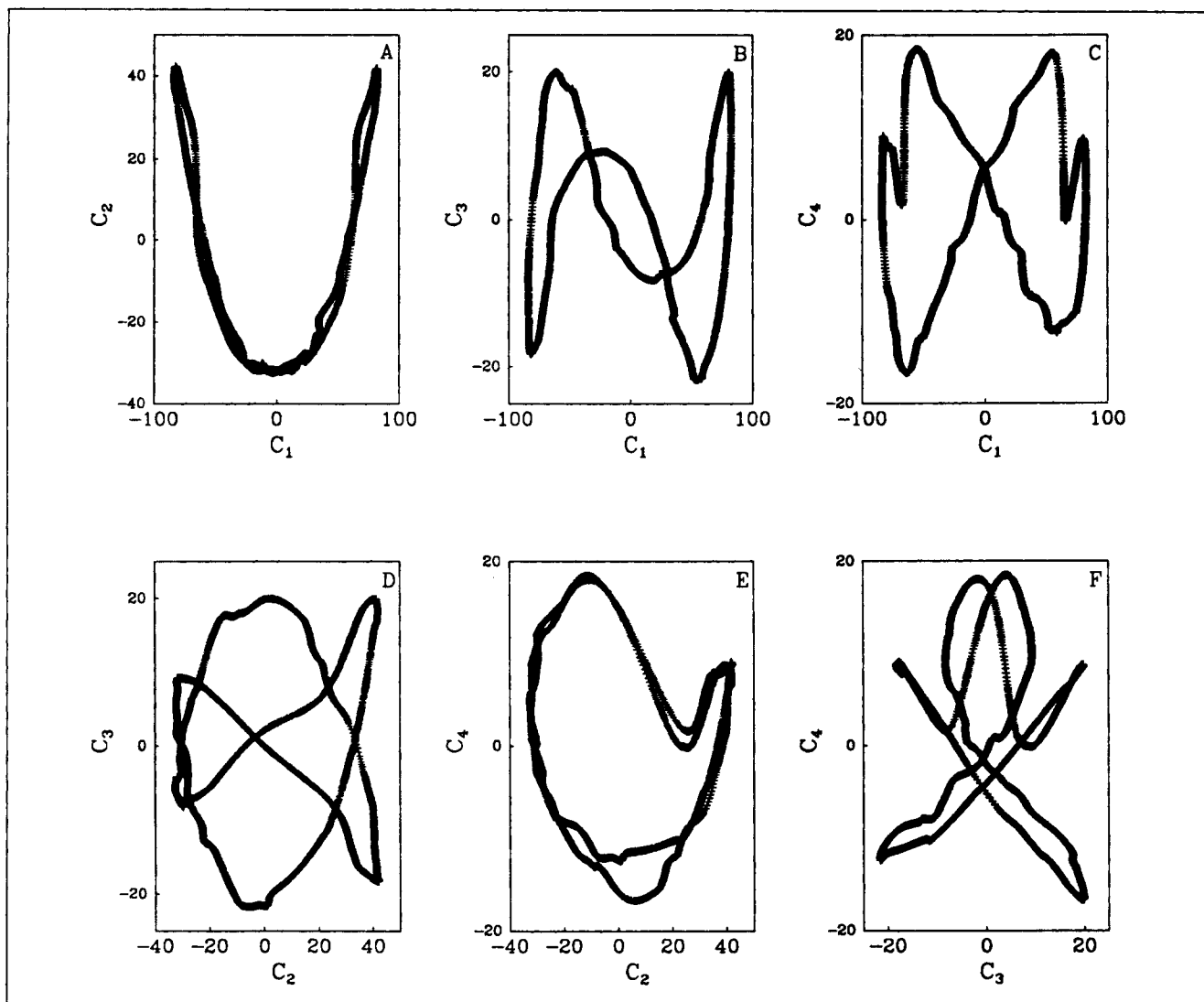
Figure 11. Different projections of the long-term prediction (attractor) of the ANN-based model (compare with Figure 6).

the instabilities and for real-time prediction and control applications of systems for which fundamental models are not available.

Literature Cited

Aubry, N. S., W.-Y. Lian, and E. S. Titi, "Preserving Symmetries in the Proper Orthogonal Decomposition," *SIAM J. Sci. Stat. Comp.*, in press (1992).

Aubry, N. S., R. Guyonnet, and R. Lima, "Spatial-Temporal Analysis of Complex Signals: Theory and Applications," *J. Stat. Phys.*, **64**, 683 (1991).

Chen, C.-C., and H. C. Chang, "Accelerated Disturbance Damping of an Unknown Distributed System by Nonlinear Dominant-Mode Feedback," *AIChE J.*, **38**, 1461 (1992).

Chen, L.-H., M. Cheng, and H. C. Chang, "Stabilization of Nonlinear Draw Resonance by the Karhunen-Loève Procedure," paper No. 238e, AIChE Meeting, Chicago (1990).

Deane, A. E., I. G. Kevrekidis, G. E. Karniadakis, and S. A. Orszag, "Low-Dimensional Models for Complex Geometry Flows: Application to Grooved Channels and Circular Cylinders," *Phys. Fluids A*, **3**(10), 2337 (1991).

Eiswirth, R. M., K. Krischer, and G. Ertl, "Nonlinear Dynamics in the CO-Oxidation on Pt Single Crystal Surfaces," *Appl. Phys. A*, **51**, 79 (1990).

Ertl, G., "Oscillatory Catalytic Reactions at Single-Crystal Surfaces," *Adv. Cat.*, **37**, 213 (1990).

Gay, D. H., and W. H. Ray, "Identification and Control of Linear Distributed Parameter Systems Through the Use of Experimentally Determined Singular Functions," *IFAC Symp. on Control of Distributed Parameter Systems*, Los Angeles (1986).

Gay, D. H., and W. H. Ray, "Application of Singular Value Methods for Identification and Model Based Control of Distributed Parameter Systems," *IFAC Symp. on Model-Based Control*, Atlanta (1988).

Hudson, J. L., M. Kube, R. A. Adomaitis, I. G. Kevrekidis, A. S. Lapedes, and R. F. Farber, "Nonlinear Signal Processing and System Identification: Applications to Time Series from Electrochemical Reactions," *Chem. Eng. Sci.*, **45**, 2075 (1990).

Jakubith, S., H. H. Rotermund, W. Engel, S. A. von Oertzen, and G. Ertl, "Spatiotemporal Concentration Patterns in a Surface Reaction: Propagating and Standing Waves, Rotating Spirals and Turbulence," *Phys. Rev. Lett.*, **65**, 3013 (1990).

Kellow, J. C., and E. E. Wolf, "Propagation of Oscillations During Ethylene Oxidation on Rh/SiO_2 Catalysts," *AIChE J.*, **37**, 1844 (1991).

Lapedes, A. S., and R. F. Farber, "Nonlinear Signal Processing Using Neural Networks: Prediction and System Modeling," Los Alamos Report LA-UR 87-2662 (1987).

Lorenz, E. N., "Statistical Forecasting Program: Empirical Orthogonal Functions and Statistical Weather Prediction," Scientific Report 1, Dept. of Meteorology, Massachusetts Institute of Technology (1956).

Lumley, J. L., *The Structure of Inhomogeneous Turbulent Flows, Atmosphere Turbulence and Radio Propagation*, p. 166, A. M. Yaglom and V. I. Tatarski, eds., Nauka, Moskow (1967).

McAvoy, T. J., N. S. Wang, S. Naidu, N. V. Bhat, J. Gunter, and M. Simmons, "Interpreting Biosensor Data Via Back Propagation," *Proc. Int. Joint. Conf. Neural Networks*, **1**, 227 (1989).

Packard, N. H., J. P. Crutchfield, J. D. Farmer, and R. S. Shaw, "Geometry from a Time Series," *Phys. Rev. Lett.*, **45**, 712 (1980).

Rico-Martínez, R., K. Krischer, I. G. Kevrekidis, M. C. Kube, and J. L. Hudson, "Discrete- vs. Continuous-Time Nonlinear Signal Processing of Cu Electrodissolution Data," *Chem. Eng. Comm.*, **118**, 25 (1992).

Rotermund, H. H., W. Engel, S. Jakubith, A. von Oertzen, and G. Ertl, "Methods and Application of UV Photoelectron Microscopy in Heterogeneous Catalysis," *Ultramicroscopy*, **36**, 164 (1991).

Sirovich, L., and C. H. Sirovich, "Low Dimensional Description of Complicated Phenomena," *Contemp. Math.*, **99**, 277 (1989).

Sirovich, L., "Turbulence and the Dynamics of Coherent Structures: I, II and III," *Quart. Appl. Math.*, **XLV**, 561 (1987).

Takens, F., "Detecting Strange Attractors in Turbulence," *Dynamical Systems and Turbulence*, D. A. Rand and L. S. Young, eds., *Lect. Notes in Math*, p. 366, Springer, Heidelberg (1981).